POSIVA-96-05

Seismic emissions induced by the excavations of the rock repository in Loviisa

Jouni Saari
IVO International Ltd

June 1996

POSIVA OY
Annankatu 42 D, FIN-00100 HELSINKI, FINLAND
Phone (90) 228 030 (nat.), (+358-0-) 228 030 (int.)
Fax (90) 2280 3719 (nat.), (+358-0-) 2280 3719 (int.)

ISBN 951-652-004-9
ISSN 1239-3096

Posiva-raportti – Posiva report

Posiva Oy
Annankatu 42 D, FIN-00100 HELSINKI, FINLAND
Puh. (90) 2280 30 – Int. Tel. +358 0 2280 30

Raportin tunnus – Report code
POSIVA-96-05

Julkaisuaika – Date
June 1996

Tekijä(t) – Author(s)
Jouni Saari
IVO International Ltd

Toimeksiantaja(t) – Commissioned by
Posiva Oy

Nimeke – Title

SEISMIC EMISSIONS INDUCED BY THE EXCAVATIONS OF THE ROCK REPOSITORY IN LOVIISA

Tiivistelmä – Abstract

The low and intermediate level waste from the Loviisa nuclear power plant will be disposed of in the bedrock of Hästholmen, in Loviisa. Two field experiments were conducted to examine the stability and structure of the rock mass surrounding the repository and its access tunnel. In addition, it was evaluated to what extent it is possible to observe the excavation induced behaviour of the Precambrian bedrock by means of a seismic emission method.

Altogether 40 induced microearthquakes were located. These events revealed structures of fractured rock within 50 metres from the excavation. Mostly the events verified the already existing 3D rock model of Hästholmen. Some observations extended and adjusted the modelled fracture geometry.

The sequences of seismic emission can determine the plane surface. Three microearthquake sequences were observed. They illustrated quite clearly the fracture geometry as well as the mechanism of the strain release.

The events induced by the excavation of the access tunnel were related to horizontal weakness zones. The events induced by the excavation of the repository seem to be associated with right-lateral strike-slip movement in the set of vertical fractures running in the direction SW-NE.

ISBN
ISBN 951-652-004-9

ISSN
ISSN 1239-3096

Sivumäärä – Number of pages
19

Kieli – Language
English

Posiva-raportti – Posiva report

Posiva Oy
Annankatu 42 D, FIN-00100 HELSINKI, FINLAND
Puh. (90) 2280 30 – Int. Tel. +358 0 2280 30

Raportin tunnus – Report code
POSIVA-96-05

Julkaisuaika – Date
Kesäkuu 1996

Tekijä(t) – Author(s)
Jouni Saari
IVO International Oy

Toimeksiantaja(t) – Commissioned by
Posiva Oy

Nimeke – Title

LOVIISASSA LOUHITUN KALLIOTILAN INDUSOIMAT SEISMISET EMISSIOT

Tiivistelmä – Abstract

Loviisan ydinvoimalaitoksesta tuleva matala- ja keskiaktiivinen jäte sijoitetaan Loviisaan Hästholmenin kallioperään. Loppusijoitustilaa ja sen yhdystunnelia ympäröivän kalliomassan stabiilisuutta ja rakennetta tarkasteltiin kahden kokeen avulla. Lisäksi selvitettiin kuinka paljon louhinnan indusoimia vaikutuksia prekambrisessa peruskalliossa voidaan havaita seismiseen emissioon perustuvan menetelmän avulla.

Mittausten aikana havaittiin 40 indusoitunutta mikromaanjäristystä. Nämä havainnot toivat esiin kallion rikkonaisuusrakenteita 50 metrin säteellä louhitusta tilasta. Useimmat havainnoista varmensivat jo olemassaolevaa Hästholmenin kallioperän kolmidimensionaalista tulkintaa. Jotkut tapaukset laajensivat kalliomallia tai aiheuttivat muutoksia mallinnettujen rakenteiden geometriassa.

Sarja mikromaanjäristyksiä voi määrittää tason pinnan. Kokeen aikana havaitut kolme maanjäristyssarjaa toivat esiin varsin selvästi siirrostason geometrian ja sen miten jännityksen laukeaminen tapahtui.

Ajotunnelin louhinnan indusoima seismisen emissio liittyi loivakaateisiin heikkousvyöhykkeisiin. Loppusijoitustilan louhinnan aiheuttamat seismiset tapaukset näyttävät liittyvän oikeakätiseen vaakasiirrokseen, joka tapahtui joukossa lounas-koillinen suuntaisia pystyrakoja.

ISBN
ISBN 951-652-004-9

ISSN
ISSN 1239-3096

Sivumäärä – Number of pages
19

Kieli – Language
Englanti

TABLE OF CONTENTS

page

Abstract

Tiivistelmä

1 INTRODUCTION 1

2 THE DATA 3

2.1 Data acquisition 3

2.2 Data analysis 3

3 INDUCED FAULT MOVEMENTS 6

3.1 Horizontal fracture zones R1 and R2 6

3.2 Vertical fracture sets R5 and R6 12

4 DISCUSSION AND CONCLUSIONS 16

5 REFERENCES 19

1 INTRODUCTION

Excavation induced seismicity has been known for centuries. Generally, the interest in this phenomena has been related to the safety and productivity of the mining industry. However, seismological techniques provide information of rock properties, stresses, fractures and mechanisms of failure for all those areas where seismic events are generated. In this study, the structure of the rock mass surrounding the excavated space, its stability and the fault geometry, are evaluated by means of excavation induced seismicity.

The excavation of a repository leads to a redistribution of in-situ stress field in the surrounding rock masses. Firstly, the explosion pushes the walls, and microcracks will arise. Later, the rock is affected by the interaction between disturbed and undisturbed rock, the cavern itself and the changes taken place in the conditions of the groundwater flow. Under these circumstances, the rock tries to release the stresses disturbing its balance, which may occur either by creeping or as a sudden stress release, which radiates seismic waves. This event is called a rockburst or an induced earthquake or, when it is audible, an acoustic emission.

The stress release takes place at certain points where the stresses exceed the strength of the rock material. The source of the seismic emission can be located by a seismic network. The events are likely to occur in weakness zones, which are also potential pathways for water flow and transport routes of dissolved radionuclides. The location and stability of these zones is an essential input for the safety analyses of a repository for nuclear waste.

The occurrence of gently dipping or horizontal fracture zones in crystalline rock is well known. However, it is rather difficult to detect these zones with ground geophysical methods. Also, since the site investigations involve drilling of a limited number of deep boreholes, most of the zones occur only in one or two cored boreholes. It may therefore be difficult to determine if an altered section of the core corresponds to a fracture zone, or not, and still more difficult to correlate a possible fracture in one borehole with one or several possible zones in other boreholes (Andersson, 1993). Of course, some vertical weakness zones as well as small subsurface fraction of fractured rock may remain undetected in borehole and surface investigations. The accurate location of induced seismic emissions offers an independent method for verifying the location of fractured rock detected or not detected by other methods.

The low- and intermediate level reactor waste of the Loviisa nuclear power plant will be disposed of in the bedrock of the island of Hästholmen (Fig. 1-1). The structure of the rock mass is dominated by three gently dipping fracture zones called the upper, lower and intermediate fracture zones (Anttila, 1988). The repository is located between the upper fracture zone and the intermediate fracture zone.

This report deals with the applicability of the induced seismic emission method in structural investigations of Precambrian crystalline rock. Two different phases of excavation were monitored to get information about the modelled horizontal zones and possible new structures. The first experiment was performed when the excavation of the access tunnel penetrated through the upper fracture zone. During the second experiment, the caverns for maintenance waste were under excavation. The report summarises the experiences gained during the investigations.

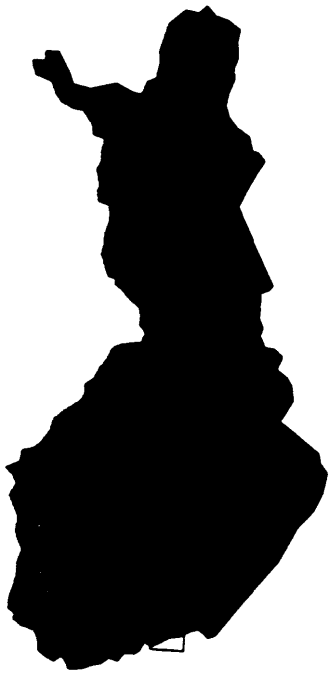

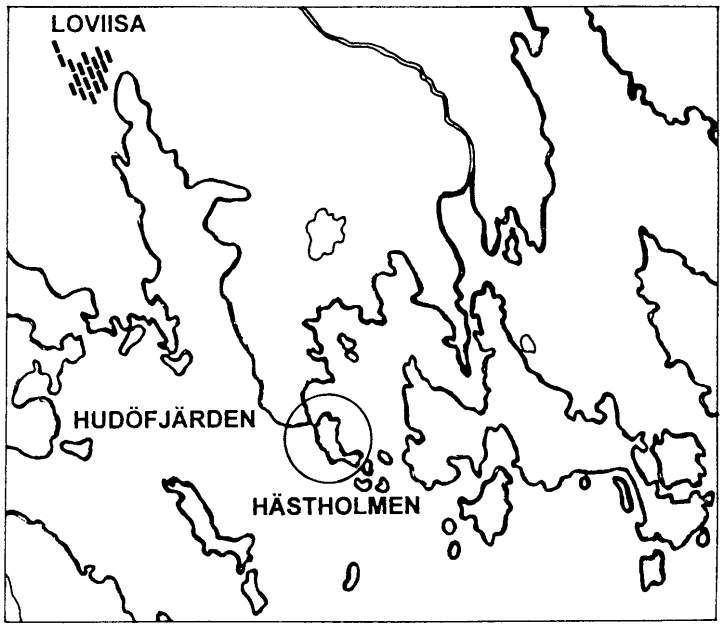

LOVIISA REGION

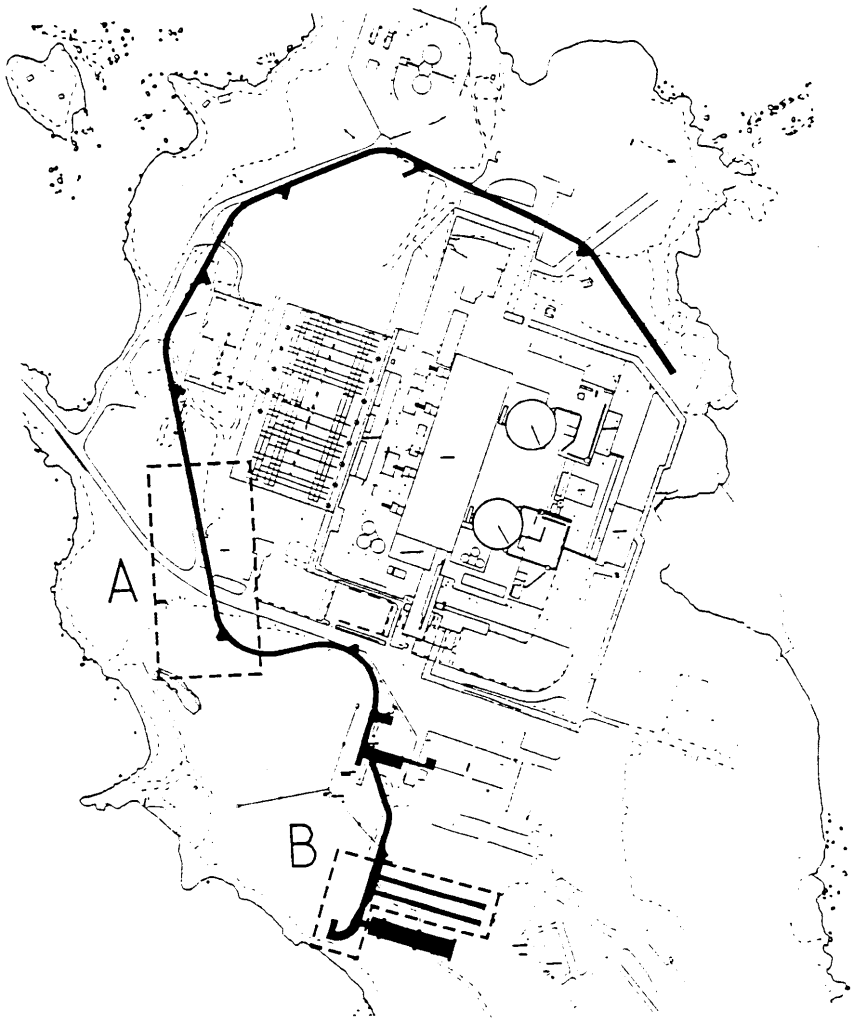

Fig. 1-1. Location of the area of study. The access tunnel goes down gently around the power plant to the depth of 110 metres. The sections under excavation during the first (A) and second (B) experiment are outlined by dashed lines.

2 THE DATA

2.1 Data acquisition

The data acquisition equipment of 16 channels was the same during both experiments. The event detector started data recording when the threshold value 2–9 mg) was exceeded. The 400 ms long event recording was sampled with 5 MHz digitiser. The triggering channel and the triggering threshold varied depending on the location of excavations. The aim was to keep the triggering level just above the noise level caused by drilling, injection and loading.

A good location accuracy was the main demand for the arrangement of the monitoring. It was assumed that most of the hypocentres are located near the excavation. To get clear onsets, each channel was preamplified relative to the presumed hypocentral distance, before digitising. The disadvantage of this was, that most of the largest amplitudes were cut, because of the 12-bit resolution of the data acquisition equipment. The amplitude information was generally lost. The accuracy of the arrival-time picks was from ±0.2 to ±0.4 ms.

There were only few boreholes available for seismic purposes. Triaxial borehole accelerometers were used because of the good quality of the recordings and to improve the location accuracy in vertical direction. The setting of the surface geophones was planned to improve the location accuracy in general and in certain interesting areas like the western side of the access tunnel.

The network geometry was planned primarily to locate the microearthquakes near the excavation. The radius of the network was of the order of 200 metres in the two experiments. The triaxial accelerometers were installed in boreholes in intact rock. The depths of the sensors ranged from 25 to 70 metres. The network was completed with vertical surface geophones, which were installed in two to four metres deep boreholes to avoid the uppermost fractured rock.

During the first experiment, the network consisted of four borehole accelerometers and four surface geophones. During the second experiment, the number of receivers was increased from eight to ten. The network consisted of three borehole receivers and seven surface geophones. The number of borehole receivers was decreased, because of the damage caused by the saline water. Numerous breaks in the operation of the borehole receivers decreased significantly the location accuracy of the network (see Chapter 5).

2.2 Data analysis

The identification of induced seismicity was made simply by comparing time and location of the observed events with the contractors catalogue of explosions. The explosions from various locations were used to calibrate the local P-wave velocity model and to estimate the location accuracy.

The average velocity (v_i) between the point of explosion and each of the receivers was calculated simply by the equation:

$$v_i = (R_i - R_N)/(T_i - T_N)$$

where R_i is the distance from the explosion to receiver *i* and T_i is the onset time at receiver *i*. The corresponding values at the borehole sensor near the explosion are denoted by symbols R_N and T_N. The average P-wave velocity (v_P) was from 5.9 to 6.0 km/s for the borehole accelerometers and from 5.4 to 5.9 km/s for the surface geophones. The lowest velocities seemed to appear, when the upper fracture zone or the excavated space was between the source and the receiver. Generally, the S-phase was impossible to observe, because of the coda of the P-phase.

Figure 2-1 shows an example of the recordings of an explosion. One can see the clear onsets in each channel as well as the individual charges of the explosion sequence in the recording of the nearest borehole accelerometer (Channel 1).

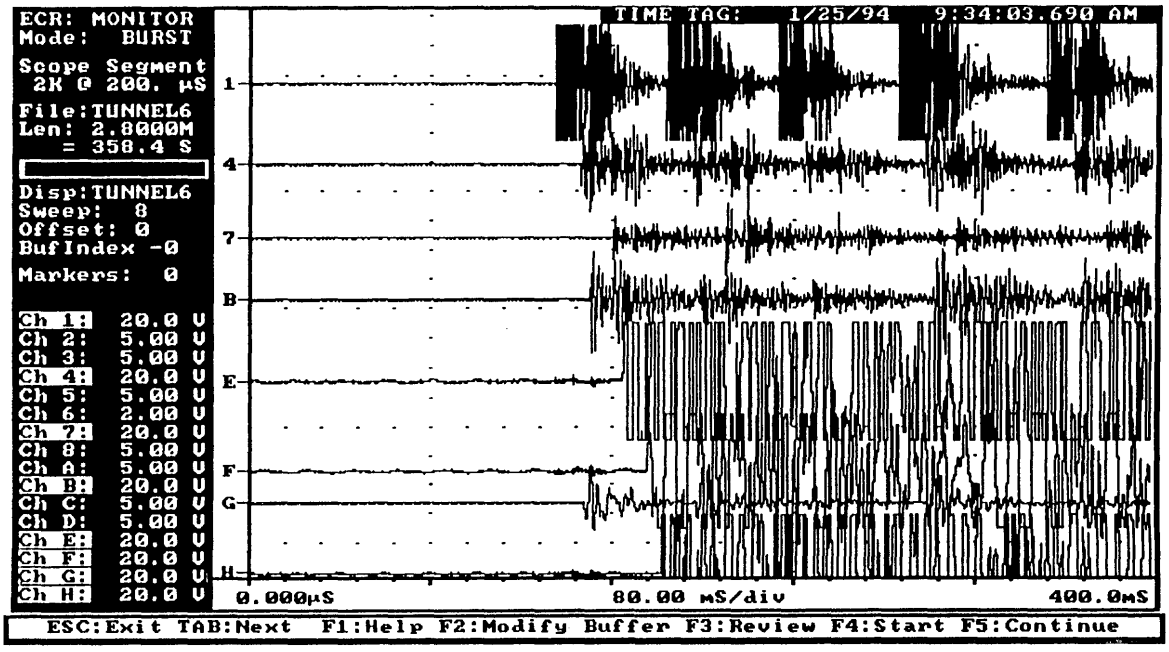

Fig. 2-1. An explosion on 25 Jan. 1994 in the access tunnel. The three uppermost recordings are from the borehole receivers and the remaining five are from surface geophones. The calculated location accuracy of this event was in the horizontal (x- and y-axis) direction ±2 m and in the vertical direction ±5 m (z-axis). The real location error was 2 metres in x-direction, 1 metre in y-direction and 2 metres in z-direction.

The standard FASTHYPO location program (Herrmann, 1979) was modified for the purposes of this study. The rock mass was described by a constant velocity model. The variation of the P-wave velocity was taken into account by using smaller weights for the surface receivers when the solution of the hypocentre was calculated. Generally, the velocity v_P=5.8 km/s was used. Depending on the location of the recordings available, also other velocities from 5.7 to 5.9 km/s were used.

The approximated location accuracy, based on the explosion data, was ±5 metres in horizontal and ±10 metres in vertical direction. The presented error estimate is conservative, representing more the calculated than the real location error. Generally, the real location errors of explosions were about half of the calculated errors. The vertical location accuracy was improved by using only the borehole recordings and the nearest surface recordings to re-evaluate the depth of the source of seismic emission. The results were discussed in the frame of three dimensional rock model of Hästholmen.

3 INDUCED FAULT MOVEMENTS

3.1 Horizontal fracture zones R1 and R2

During the first experiment, from 15 Nov. 1993 to 1 March 1994, about 200 metres of the access tunnel was excavated. The height of the tunnel is 8 metres and the width 6 metres. At the depth of 90 metres, the tunnel passes through the five to ten metres thick upper fracture zone (R1) (Figure 3-1). The tunnel curves eastwards just after passing through zone R1. The intermediate fracture zone R2 stays below the excavated space.

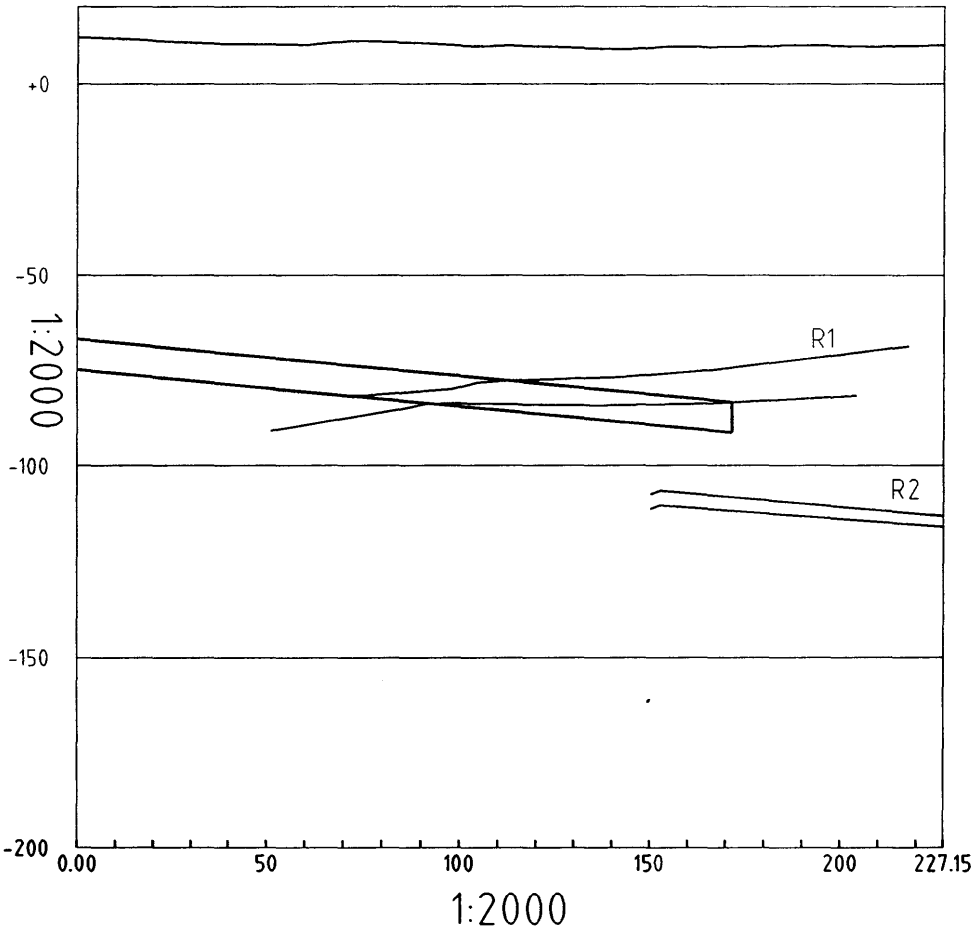

Fig. 3-1. The cross-section along the access tunnel. The location of the upper fracture zone and the intermediate fracture zone are denoted by symbols R1 and R2. The fracture zones are presented as far as they were known before the excavation.

Besides the intersection of the access tunnel and the upper fracture zone, there was another primary source of interest. The network was also designed to extract the fracture model at the western side of the tunnel where the upper fracture zone is gently arising towards the bottom of the sea. In that area, the location of the subsurface structures was uncertain.

The purposes of the first experiment were to investigate the seismic emission method and to find out:

- How fracture zone R1 and the remaining rock mass respond to the excavations?
- To what extent the upper fracture zone is disturbed?
- Is it possible to verify or improve the existing fracture model?
- Is there, possibly, a connection between the upper fracture zone and the sea?

Altogether 25 microearthquakes were located during the measurements. The location accuracy of 19 events was good, i.e. ±5 metres in horizontal and ±10 metres in vertical direction. They were located by using 6 to 8 accurate onset readings. The location accuracy of 6 events was only sufficient. In these cases there were only 3 to 5 readings available or, for some reason, the iteration process of the location program did not converge.

Like the events in Figure 3-2, the seismic emissions often occurred in sequences near the excavation area. At the time of this example, the excavation was on the upper surface of fracture zone R1. The events occurred on the lower surface of the same fracture zone.

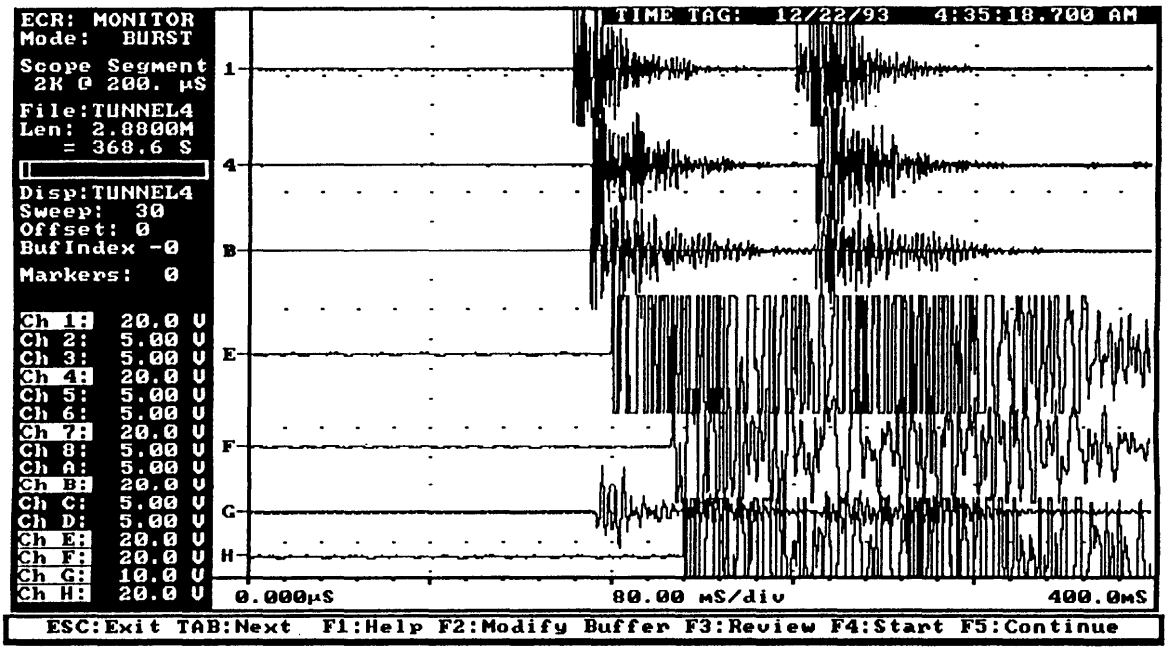

Fig. 3-2. Two induced microearthquakes of 22 Dec. 1993 on the lower surface of fracture zone R1. See the good quality of the three uppermost recordings (borehole accelerometers) compared to the four lowermost recordings (surface geophones).

As expected, the events occurred mostly within ten metres from the tunnel (Figure 3-3). However, there are few exceptions. The furthermost microearthquake occurred 50 metres from the tunnel, already before the excavation reached the fracture zone. This event occurred 40 metres NW from the modelled area of the rock mass and extended the 3D-rock model remarkably. The event (Event A in Fig. 3-4) seems to have occurred in the lower surface of fracture zone R1. In Figure 3-6, the event is the northernmost one. This rockburst, and the fact that the upper fracture zone does not intersect the borehole Y17, indicate that

the upper fracture zone is likely to run horizontally to the west and remain below the sea bottom, at least, in the near vicinity of Hästholmen.

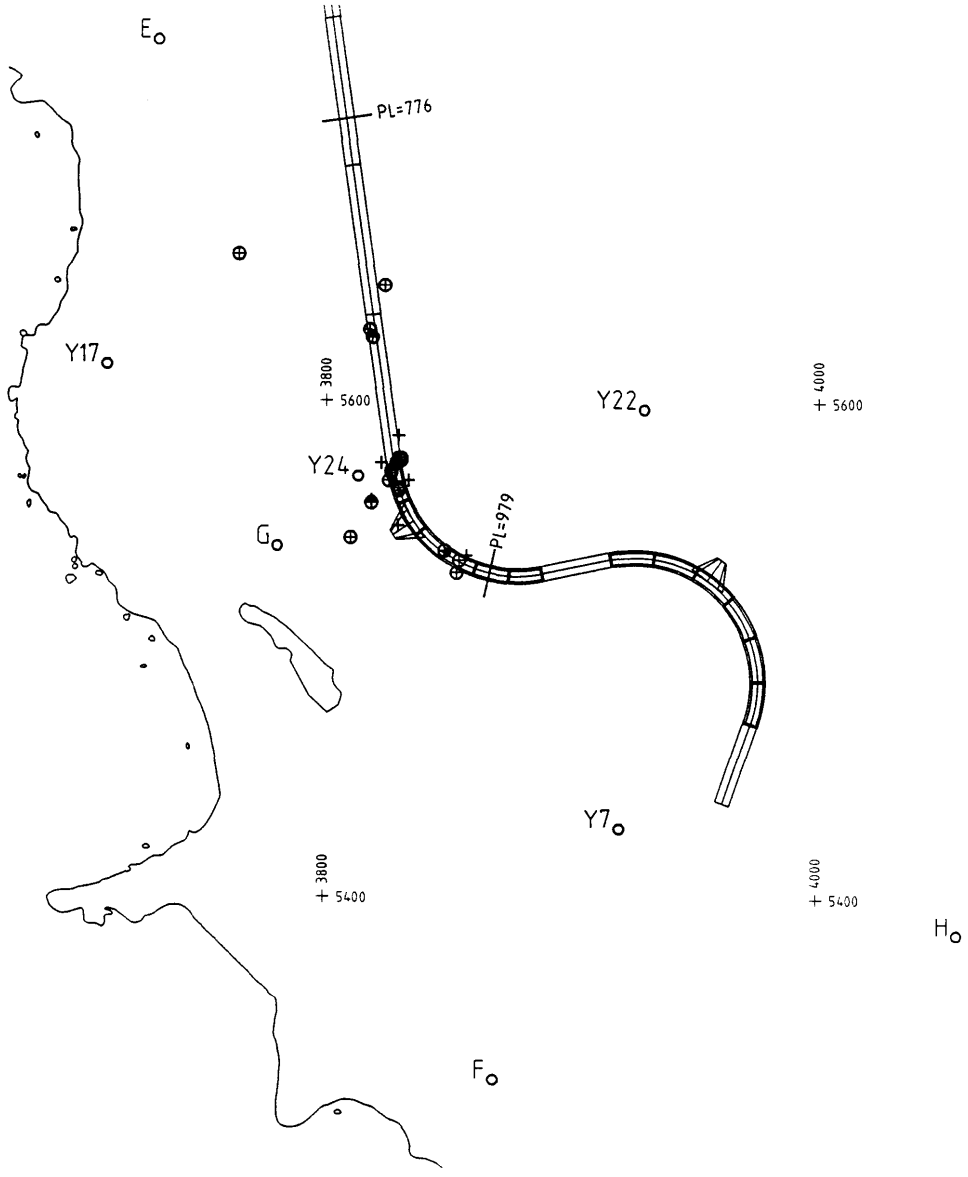

Fig. 3-3. The access tunnel and induced seismicity. Well located events are denoted by the circled crosses (⊕), the sufficient locations by pure crosses (+) and the receivers by open circles (O). The accelerometers were in boreholes Y7, Y17, Y22 and Y24 and the surface geophones at points E-H. The excavated section of the tunnel is between lines PL=776 and PL=979. The local co-ordinate system is presented in metres.

The interpretation of induced earthquake sequences is much more reliable than the interpretation of single events. The orientation of the weakness zone can be determined independently, without any previous knowledge of the structures. For example, the sequences observed during the two experiments define quite clearly the fracture geometry as well as the proceeding of the strain release.

On 21 Feb. 1994, a sequence of six microearthquakes proceeded a trip of 42 metres in 12 seconds. It determined a structure about ten metres below the tunnel and the upper fracture zone. The proceeding of the hypocentres from NW to SE is most easily seen by comparing the relative onset times (Fig. 3-5) at channels 7 and B (boreholes Y7 and Y17 in Fig. 3-3). Based on this sequence and the visual observations in the tunnel, the location of the fracture zone R2 was adjusted.

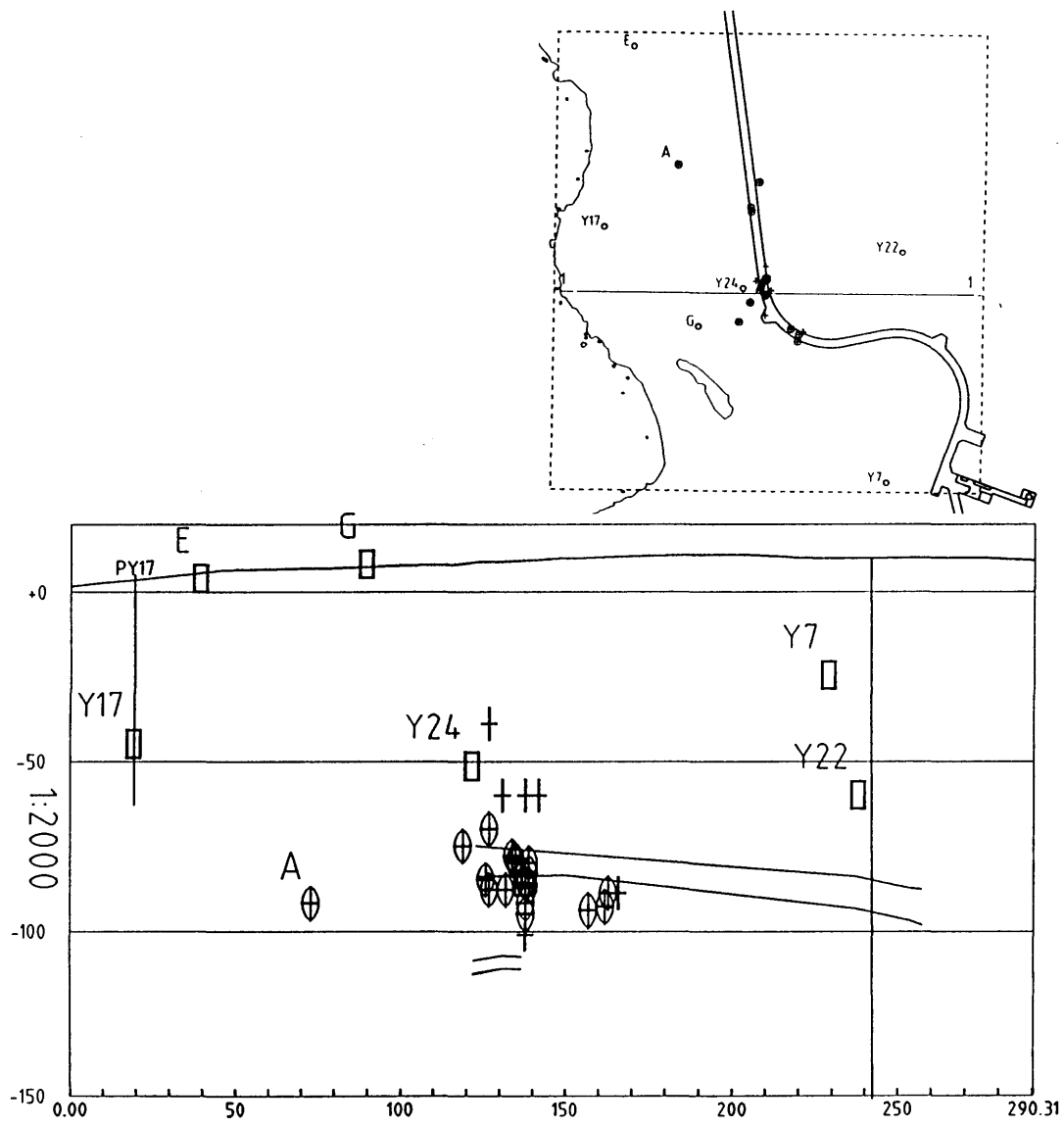

Fig. 3-4. Profile 1-1 crossing the access tunnel and structures R1, R2 and R5 (western side of it). View looking north. The receivers and hypocentres inside the dashed line of the map are included. Well located hypocentres are denoted by a cross surrounded by an ellipse and sufficient locations by a pure cross. The tunnel is just in the middle of the cluster of hypocentres. The accelerometers and the geophones are shown as quadrangles and drill hole Y17 is shown as a vertical line.

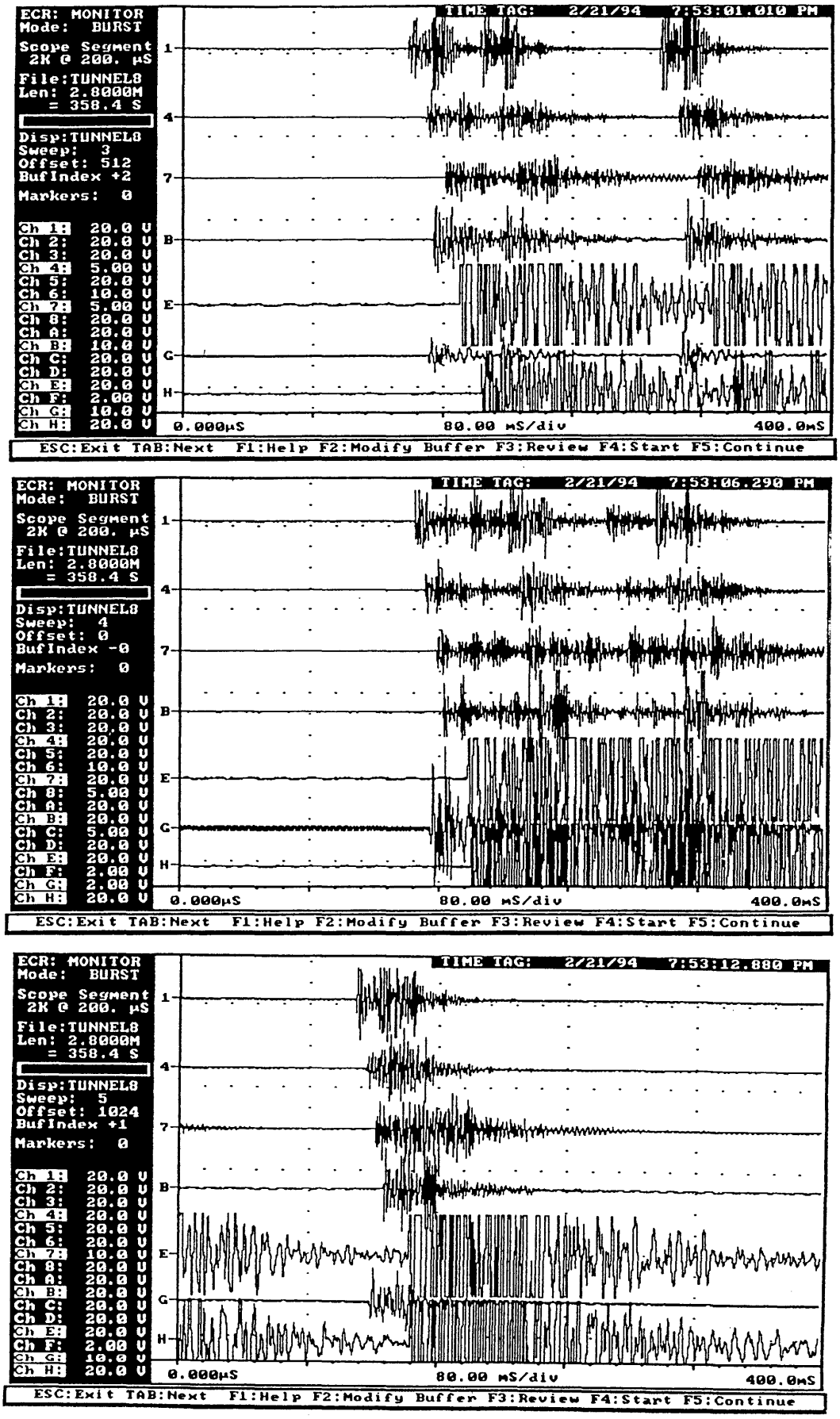

Fig. 3-5. The microearthquake sequence of 21 Feb. 1995. Recordings at 7:53:01.0 PM, 7:53:06.3 PM and 7:53:12.9 PM. The four uppermost channels are from the boreholes and the three lowermost are from the surface.

During the microearthquake sequence of 28 Jan. 1994, the rupture proceeded more slowly. Four microearthquakes occurred within eight hours. Their hypocentres moved 28 metres along the upper surface of fracture zone R1 (from a_1 to a_4 in Fig. 3-6). The preceding explosion was exploited below the fracture zone eight hours before the first induced seismic (a_1) emission occurred.

Generally, seismic emission occurred in the upper or in the lower surface of fracture zone R1 (Fig. 3-6). The events below the tunnel and R1 are related to R2 and occurred during the above mentioned earthquake sequence. The events significantly above the fracture zone are not accurately located.

The inaccurate locations indicate anomalous velocities between the seismic source and the receivers. One or more of the readings do not fit the constant velocity model. This may be a consequence of fractured rock or the excavated tunnel disturbing the normal travelling of the seismic signal. However, there were too few readings to rule out the inaccurate readings and to re-locate the events. This was the reason to increase the number of receivers in the second experiment.

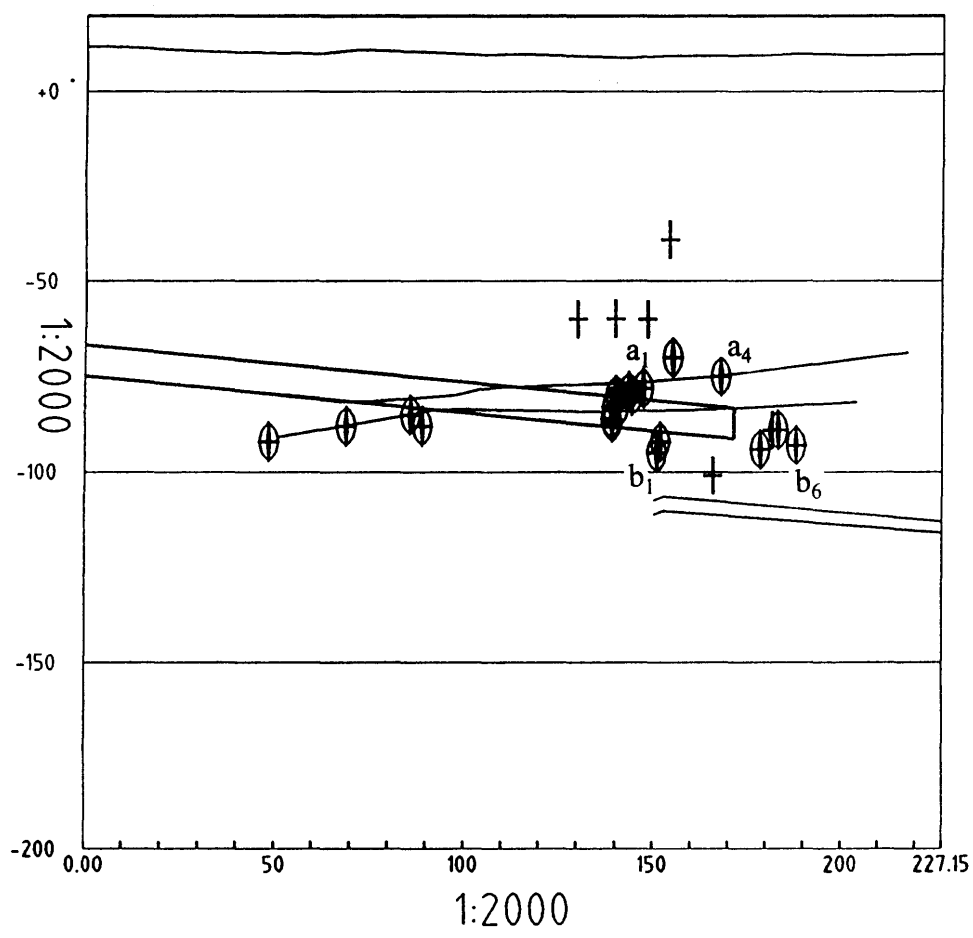

Fig. 3-6. Profile along the access tunnel (see Fig. 3-1). View looking normal to the tunnel. Well located hypocentres are denoted by a cross surrounded by an ellipse and sufficient locations by a pure cross. The microearthquake sequences on 28 Jan. 1994 proceeded from a_1 to a_4 and on 21 Feb. 1994 from b_1 to b_6.

3.2 Vertical fracture sets R5 and R6

The second period of measurements was performed from the middle of March 1995 to the middle of June 1995, when two 100 metres long caverns for maintenance waste and the end of the access tunnel were excavated (see Fig. 1-1). The dimensions of the excavated structures are of the same order as the access tunnel. The caverns are at the depth of 110 metres.

The data acquisition equipment was basically similar to the one used in the first experiment. However, few changes were made. The number of receivers was increased to improve the location accuracy. The data processor (PC-286) was replaced by a faster one (PC-386) to reduce the processing time. In the first experiment, part of an microearthquake sequence might have been undetected, because of the five seconds long processing time between the recordings (see e.g. Fig. 3-6). However, the processing time was still about two seconds.

Two vertical sets of fractures were modelled in the area of the excavations (Fig. 3-7). Structures R5 and R6 are formed by a sparse set of narrow fractures. The mechanical properties of R5 and R6 are better, and the rock is more intact as compared to fracture zones R1 and R2.

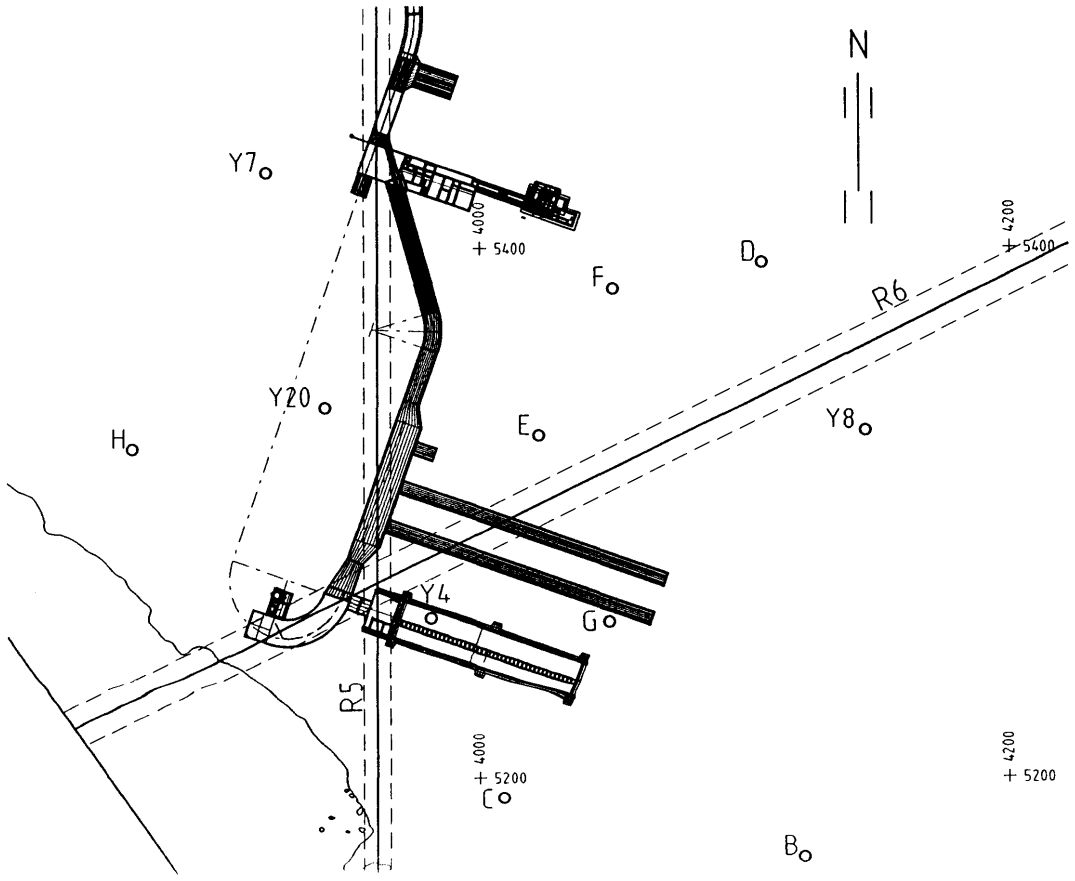

Fig. 3-7. The setting of the seismic network and the locations of the vertical sets of fractures R5 and R6. The receivers are shown as circles. The triaxial accelerometers are in boreholes Y4, Y7 and Y20 and the surface geophones at points D-H. The two northernmost caverns are for the maintenance waste. The cavern for solidified waste is south of them.

As in the first experiment, the stability and the geometry of fractures R5 and R6 and, possibly, a priori unknown fractures were studied. In addition, the aim was to use the observed rockbursts as input data for real time design of the excavations.

The background of the real time design is presented in Figure 3-8. According to the model, the upper fracture zone is ten metres above the end of the first cavern of the maintenance waste. The aim was to verify, whether the location of fracture zone R1 was modelled correctly. Some indications of induced seismicity were expected, if the real location of R1 were lower. This might have given a reason to re-evaluate the excavation methods and even to change the layout of the repository.

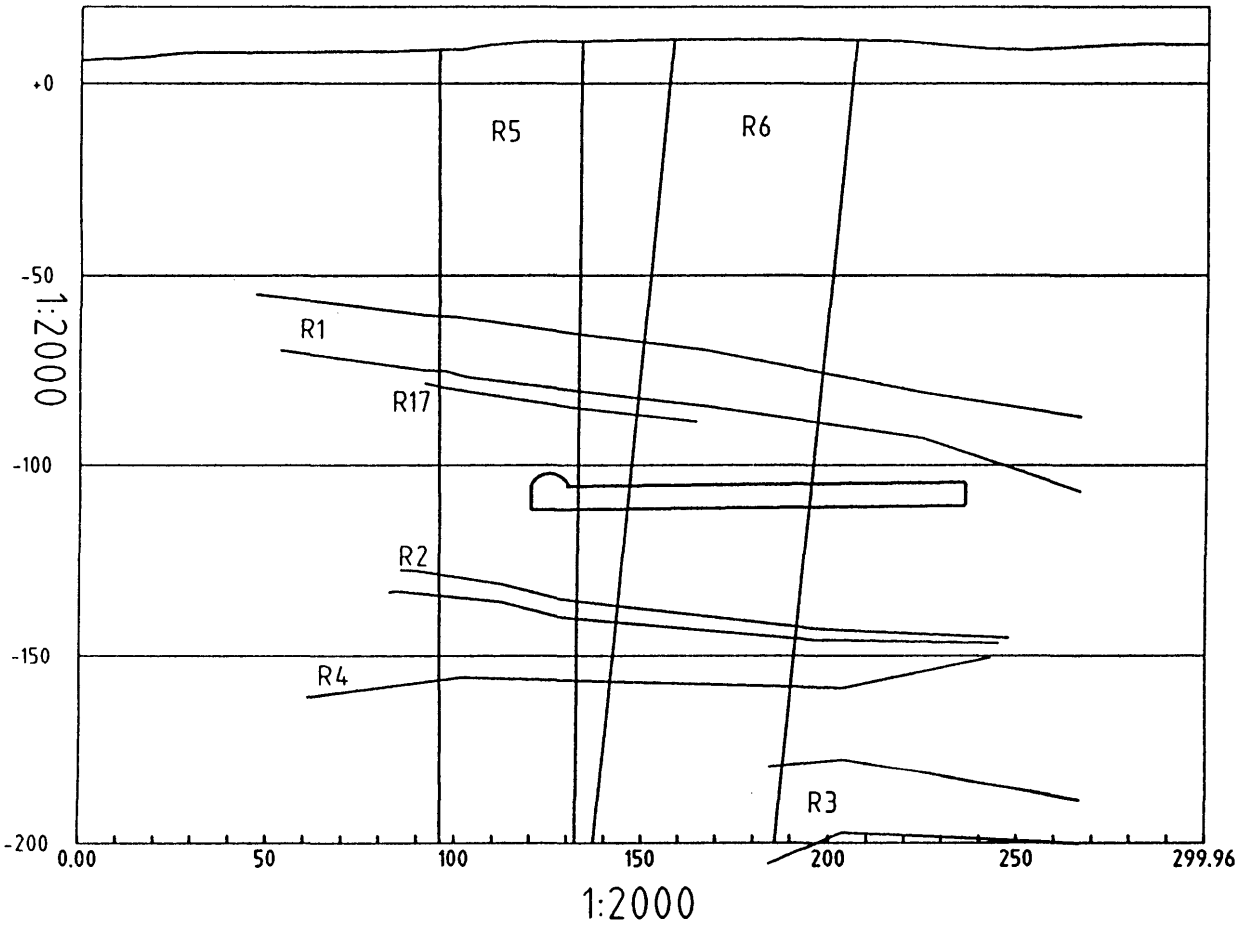

Fig. 3-8. Profile along the northern cavern for the maintenance waste.

The two clusters of epicentres are in the areas where the set of fractures R6 intersects the fractures of R5 or the caverns for the maintenance waste (Fig. 3-9). The only exception is event number 12, which is apart from the rest of events and structure R6. The seismic emissions occurred mostly near the excavations. The furthermost events, relative to the excavation, events 13 and 14 (19 May 1995), occurred 25 metres NE from the location of excavation and 20 metres from the access tunnel.

It is concluded that most of the observed induced movements are rather likely related to structure R6, and the type of the movement in that structure is evidently right lateral strike-slip. The conclusion is based on the following observations:

- The microearthquake sequence of 4 April 1995 rupture in 5 seconds a trip of 38 metres (from events 1 to event 6 in Fig. 3-9) along the north-western surface of R6.
- As mentioned above, all the events, except for event number 12, can be associated with the set of fractures in direction SW-NE.
- There are visual observations of vertical fractures in the caverns near the hypocentres. These fractures cut the entire wall and their strike coincide with the SW-NE direction.
- Before the caverns were excavated, in-situ stress measurements were performed at the end of the access tunnel. The estimated principal stresses (σ_H = 17.4 MPa, σ_h = 6.5 MPa and σ_v = 5.2 MPa) show a relatively strong horizontal compression in the direction E-W (Suomen Malmi Oy, 1994). This direction of compression is very suitable for a right-lateral strike slip in SW-NE oriented fracture set R6. On the other hand, the N-S oriented fractures (R5) are most likely compressed and stable, for the same reason.
- The induced rockburst often occurred NE from the preceding explosion (e.g. events 8 - 10 and 13 - 14) or the preceding microearthquake (e.g. events 2 - 7). This seems to indicate that the disturbance in the stress field has moved to NE.

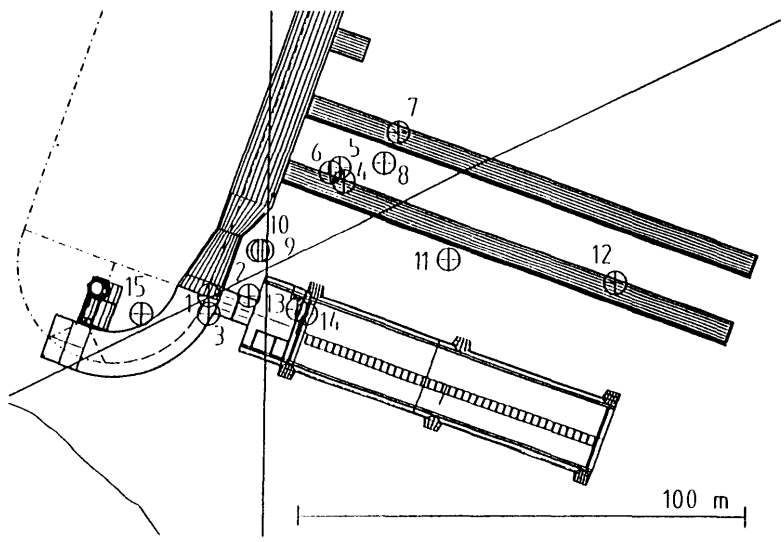

Fig. 3-9. Induced seismicity (⊕) numbered in the order of occurrence. The median lines of the about 20-metre wide fracture sets R5 and R6 are presented. The southern-most cavern was excavated after the measurements. The events in that area were induced by the excavations SW of it, in the curve of the access tunnel.

In vertical direction the deviation of hypocentres is very small (Fig. 3-10). The events are mainly at the level of excavation. Events 2, 9 and 10 are slightly above the excavation and event 12 slightly below it. Event 11, which is 10 metres diagonally below the second cavern of the maintenance waste, is most clearly distinguished from the group observations. It is

quite likely related to the vertical SW-NE oriented fracture cutting the entire wall of the cavern. The most important result shown in Figure 3-10 is that fracture zone R1 as well as fracture zone R2 remained stable during the experiment.

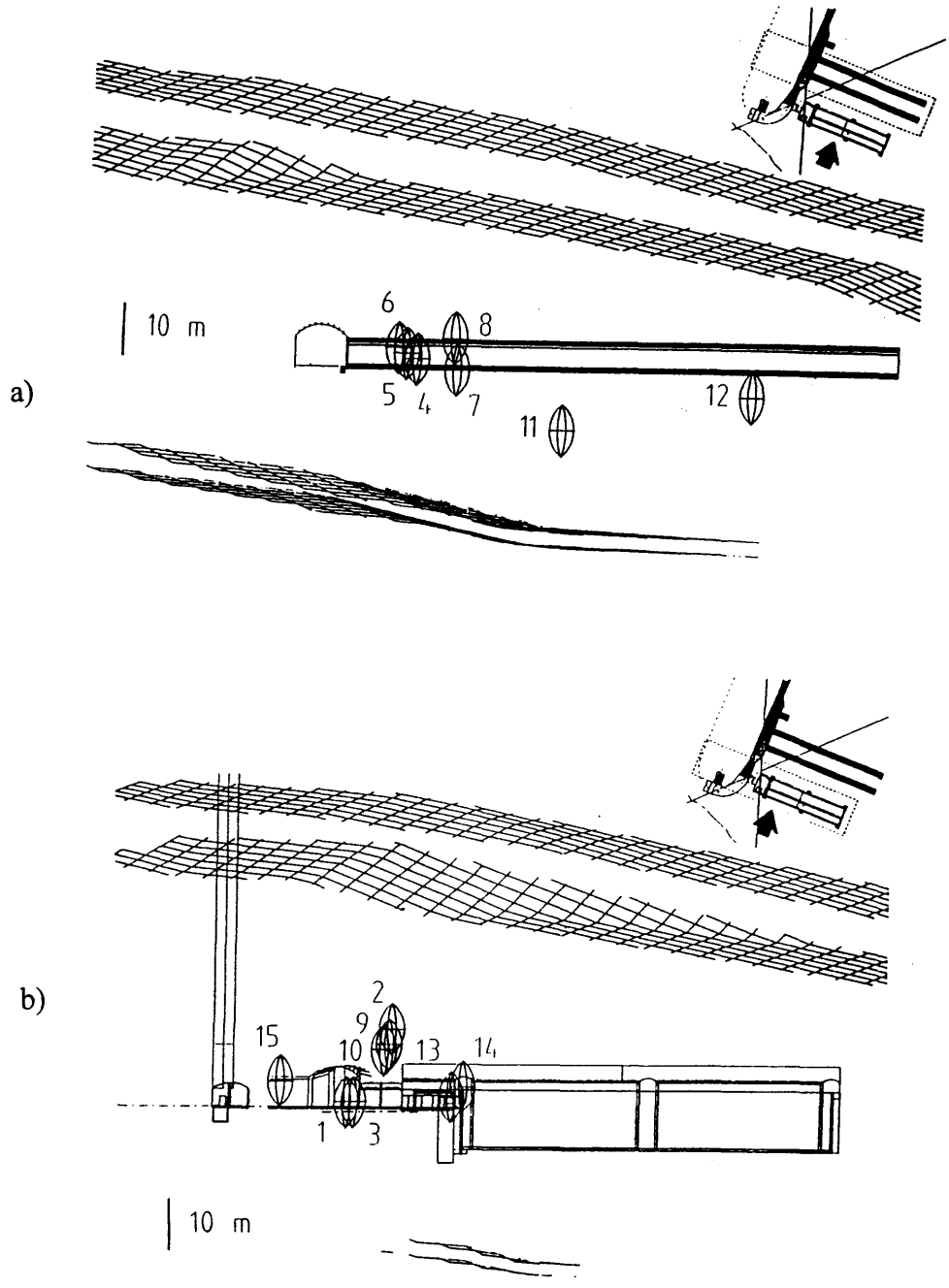

Fig. 3-10. Vertical cross-sections including the caverns for the maintenance waste (a) and the cavern for the solidified waste (b). The areas included are shown by dashed lines in the maps enclosed. The arrows illustrate the view direction. The upper and lower surfaces of R1 and R2 are shown as hatching.

4 DISCUSSION AND CONCLUSIONS

The distribution of fractures and fracture zones is an integral part of the safety analysis for the final disposal of nuclear waste. Their geometry and characteristics are very important when the ground water flow and the long term stability of the bedrock are examined. Therefore, the fracture model guiding the safety analysis should be verified by several independent methods.

The location of fracture zones is mainly interpreted by the geological and geophysical studies made on the ground surface. These investigations are generally complemented by studies in a limited number of boreholes. This might lead to misinterpretation or inaccuracy, specially, when the gently dipping fracture zones are concerned.

Altogether 40 induced microearthquakes were located during four months of measurements. As expected, most of the events occurred at the level of the excavation and within the distance of 10 metres from the structure excavated. The furthermost event was 50 metres apart from the location of the excavation. Generally, the hypocentres fitted rather well the known structures, but some observations extended or adjusted the previous rock model.

Low-magnitude excavation induced microseismic events usually cause no significant structural damage. The largest recorded amplitudes of induced microearthquakes were mostly cut, because of the 12-bit digital data acquisition system available. However, the whole amplitude range of the largest explosions and the microearthquakes were detected in the short period seismic station two kilometres north of the repository. The frequency range of the seismic station did not cover the highest frequencies of the events. This means that the estimated magnitudes were not accurate, but it can be concluded that induced events were smaller than explosions and that the magnitudes of the microearthquakes were of the order of $M_L = -1$ or smaller.

It is often difficult to identify the host event, which triggers the rockburst. The induced seismicity is primary caused by explosions but also to some extent by cement grouting and by secondary changes, such as changes in water pressure. As far the host event is correctly determined, the time difference between the host explosion and the induced event seemed to be from few seconds to few days.

During the experiments, there were relatively long quiet periods interrupted by short intervals of induced activity lasting from few seconds to few days.

The Loviisa seismic station detected induced seismicity in Hästholmen two months after finishing the excavations. At that time, the grouting of the rock was in progress, but these events might as well be a consequence of slow adjustment of the rock mass. It is likely that events occurring with a long delay after the excavations are related to interaction between the disturbed and undisturbed rock further away from the excavated structures. They might occur seldom, but their benefit to structural studies is obvious.

The experiments show that even at the depth of about 100 metres, the Finnish bedrock responds to the variations in the stress field with numerous microearthquakes, which can be detected and located accurately. The repository for spent nuclear fuel will be located at a depth of 500 metres in conditions of relatively high pressure. The volume of the disturbed

rock mass is expected to be larger than in this study. Therefore, the induced seismicity will very likely provide a large amount of information, specially, if the whole period of excavation and the few months after that are monitored. When the repository is excavated, an investment into an intelligent monitoring and analysis system should be considered to get the full benefit of the information of the induced seismic signals.

The results of this study, event detection and location, represent only a minor fraction of the information which is contained in the seismic signals. All the applications used in studies of natural born earthquakes can also be used when the induced seismicity is regarded. For example, spatial and temporal variation of the source parameters, such as stress drop or slip rate of induced seismicity, can be presented. Also the fault plane solutions are a standard part of modern systems for monitoring induced seismicity (see e.g. McGeary et al., 1992; Young et al., 1992; Urbancic and Young, 1993). This also means that the variations of the stress field can be examined and the results of the in-situ stress measurements can be verified.

The most unambiguous information of the fractures can be achieved by the analysis of the induced earthquake sequences. Therefore it is recommended that, in future investigations, the processing system should be fast enough to record all the events of an sequence. In this study, three earthquake sequences determined 30 - 40 metres long sections of faults. The earthquake sequences are of special value also when the stress field and the disturbances proceeding in it are investigated.

Quite often microearthquakes and, specially, microearthquake sequences turn out to be a spread over a plane surface. The location accuracy of these events can be improved remarkably by the relative location method. The relative location technique minimises the inaccuracy of the locations and the fault plane can be determined more precisely than by conventional methods (e.g. Slunga et al., 1995; Saari and Slunga, 1996). Also the orientation of the stress released and other parameters characterising the fault can be estimated more reliably by a simultaneous analysis of the events related to the same fault.

The fault plane solution for an earthquake determines two orthogonal planes. One of these determines the real fault plane and the other one, the auxiliary plane, has no physical existence. The correct fault plane can be chosen, if the other fault plane orientation coincides with a known fault or if the hypocentres of the earthquakes determine a plane surface. The advantage of the latter method is that it is not necessary to have a priori knowledge of the weakness zones in the bedrock.

One of the objectives of this study was to get experiences of the induced seismic emission method as a tool for structural investigations. It can be concluded that the seismic emissions induced by excavations can be used:

- To locate weakness zones and to approximate their stability.
- To verify and to re-evaluate, in an independent way, the existing rock model.
- To bring out completely new weakness zones undetected in previous studies.
- To verify the orientation of the stress field determined by the in-situ measurements.
- To illustrate the space-time variation of different parameters (stress drop, peak slip, seismic moment, stress orientation, etc.) of induced seismicity.

By modern applications, most of the above mentioned results characterising the rock mass can be achieved almost in real time. This means that the seismic emission observations can be used to bring out the need of additional drilling or other investigations even during the excavation. These studies may result in the choosing of an altered excavation method or even in the adjustment of the layout of the repository.

5 REFERENCES

Andersson P. (ed.), 1993. The Fracture Zone Project - Final report. SKB Technical Report, TR 93-20.

Anttila P., 1988. Engineering geological conditions of the Loviisa power plant area relating to the final disposal of reactor waste. University of Turku, Annales universitatis Turkuensis, Ser. A 72, 131 p.

Herrmann R.B., 1979. A hypocentre location program, Earthquake Notes, vol. 50, No. 2.

McCreary R., McGaughey J., Potvin Y., Ecobichon D., Hudyma M., Kanduth H. and Coulombe A., 1992. Results from microseismic monitoring, conventional instrumentation, and tomography surveys in the creation and thinning of a burst-prone Sill Pillar. PA-GEOPH., vol. 139, No 3/4.

Saari J. and Slunga R., 1996. Fault plane solutions of microearthquakes in the Loviisa region in south-eastern Finland. Report POSIVA-96-02.

Slunga R., Rögnvaldsson S.Th. and Bödvarsson R., 1995. Absolute and relative location of similar earthquakes in Southern Iceland. Geoph. Journ. Int., 123:409-419.

Suomen Malmi Oy - Finnexploration, 1994. Rock stress measurements at Hästholmen, Loviisa (Kallion jännitystilamittaukset Loviisan Hästholmenilla), Study Report LO-K490-47 (in Finnish).

Urbancic T.I. and Young R.P., 1993. Space-time variations in source parameters of mining induced seismic events with M <0. Bull. Seism. Soc. Am., vol. 83, No 2. pp. 378 - 397.

Young R.P., Maxwell S.C., Urbancic T.I. and Feignier B., 1992. Mining-induced micro-seismicity: Monitoring and applications of imaging and source mechanism techniques. PAGEOPH., vol. 139, No 3/4.

LIST OF POSIVA REPORTS PUBLISHED IN 1996

POSIVA-96-01
Determination of U oxidation state in anoxic (N_2) aqueous solutions – method development and testing
Kaija Ollila
VTT Chemical Technology
June 1996
ISBN 951-652-000-6

POSIVA-96-02
Fault plane solutions of microearthquakes in the Loviisa region in south-eastern Finland
Jouni Saari
IVO International Ltd
Ragnar Slunga
Försvarets Forskningsanstalt, Stockholm, Sweden
June 1996
ISBN 951-652-001-4

POSIVA-96-03
Thermal optimisation of the final disposal of spent nuclear fuel
Heikki Raiko
VTT Energy
June 1996
(In Finnish)
ISBN 951-652-002-2

POSIVA-96-04
On the origin and chemical evolution of groundwater at the Olkiluoto site
Petteri Pitkänen
Technical Research Centre of Finland
Margit Snellman
Imatran Voima Oy
Ulla Vuorinen
Technical Research Centre of Finland
June 1996
ISBN 951-652-003-0

POSIVA-96-05
Seismic emissions induced by the excavations of the rock repository in Loviisa
Jouni Saari
IVO International Ltd
June 1996
ISBN 951-652-004-9